miR-218 opposes a critical RTK-HIF pathway in mesenchymal glioblastoma

Lijoy K. Mathew[a,b], Nicolas Skuli[a,b,c], Vera Mucaj[a], Samuel S. Lee[a,b], Pascal O. Zinn[d], Pratheesh Sathyan[d], Hongxia Z. Imtiyaz[a], Zhongfa Zhang[e], Ramana V. Davuluri[e], Shilpa Rao[f], Sriram Venneti[g], Priti Lal[g], Justin D. Lathia[h], Jeremy N. Rich[i], Brian Keith[a,j], Andy J. Minn[k], and M. Celeste Simon[a,b,l,1]

[a]Abramson Family Cancer Research Institute, [b]Howard Hughes Medical Institute, [d]Penn Molecular Profiling Facility - Bioinformatics Group, and Departments of [c]Cell and Developmental Biology, [e]Pathology and Laboratory Medicine, [f]Cancer Biology, and [g]Radiation Oncology, University of Pennsylvania, Philadelphia, PA 19104; [h]Center for Systems and Computational Biology, Molecular and Cellular Oncogenesis Program, The Wistar Institute, Philadelphia, PA 19104; Departments of [i]Cellular and Molecular Medicine and [j]Stem Cell and Regenerative Medicine, Lerner Research Institute, Cleveland Clinic, Cleveland, OH 44195; [k]Department of Genetics, MD Anderson Cancer Center, University of Texas, Houston, TX 77030; and [l]Institut National de la Santé et de la Recherche Médicale U1037, Institute Claudius Regaud, 31052 Toulouse, France

Edited* by William G. Kaelin, Jr., Harvard Medical School, Boston, MA, and approved November 27, 2013 (received for review July 30, 2013)

Glioblastoma multiforme (GBM) and the mesenchymal GBM subtype in particular are highly malignant tumors that frequently exhibit regions of severe hypoxia and necrosis. Because these features correlate with poor prognosis, we investigated microRNAs whose expression might regulate hypoxic GBM cell survival and growth. We determined that the expression of microRNA-218 (*miR-218*) is decreased significantly in highly necrotic mesenchymal GBM, and orthotopic tumor studies revealed that reduced *miR-218* levels confer GBM resistance to chemotherapy. Importantly, *miR-218* targets multiple components of receptor tyrosine kinase (RTK) signaling pathways, and *miR-218* repression increases the abundance and activity of multiple RTK effectors. This elevated RTK signaling also promotes the activation of hypoxia-inducible factor (HIF), most notably HIF2α. We further show that RTK-mediated HIF2α regulation is JNK dependent, via jun proto-oncogene. Collectively, our results identify an *miR-218*–RTK–HIF2α signaling axis that promotes GBM cell survival and tumor angiogenesis, particularly in necrotic mesenchymal tumors.

Naturally occurring oxygen (O_2) gradients serve as morphogenic signals in rapidly growing embryonic tissues (1) but become extreme in pathophysiological conditions such as ischemia or solid tumors. Chronic exposure to severe O_2 deprivation frequently produces necrotic zones surrounded by densely packed, hypoxic tumor cells. This cellular architecture is a common feature of glioblastoma multiforme (GBM), highly malignant brain tumors with a median patient survival of only 12–14 mo (2). Pseudopalisading GBM cells at the periphery of necrotic areas exhibit nuclear hypoxia-inducible factor 1α (HIF1α) protein accumulation and express hypoxia-regulated genes that control angiogenesis, extracellular matrix degradation, and invasive behavior (3, 4). Recent genomic sequencing and transcriptome analyses stratified GBM into distinct subtypes, including mesenchymal and proneural (5, 6). Importantly, patients with the aggressive mesenchymal subtype exhibit a particularly high degree of tumor necrosis (6). Moreover, an independent study revealed that GBM samples with high levels of necrosis are significantly enriched for the mesenchymal transcriptional gene signature (4). In particular, hypoxic GBM cells surrounding necrotic zones express high levels of the mesenchymal transcription factors C/EBP-β and C/EBP-δ, indicating a clear association between hypoxia, necrosis, and a mesenchymal GBM cellular identity (4).

Elucidating the biological mechanisms whereby hypoxic tumor cells acquire the ability to survive and migrate under severe conditions is of significant clinical importance. Because microRNAs (miRNAs) are known to regulate complex cellular processes, including proliferation, differentiation, motility, and survival (7, 8), we investigated how specific miRNAs control growth within the GBM tumor microenvironment. Although microRNA-218 (*miR-218*) previously was shown to be repressed in GBM relative to normal brain tissue (9, 10), we determined that *miR-218* is reduced further in highly necrotic and hypoxic GBM, as compared with less necrotic samples. To delineate the role of *miR-218* repression in GBM further, we performed intracranial xenograft assays and determined that *miR-218* silencing confers chemoresistance in vivo, uncovering a role for *miR-218* repression among its previously established protumorigeneic properties. We have identified multiple components of a receptor tyrosine kinase (RTK) signaling pathway as direct *miR-218* targets and demonstrate that constitutive RTK activity reverses *miR-218*–mediated chemosensitivity in vivo. Moreover, we showed that HIFs, specifically HIF2α, function as downstream effectors of a low *miR-218*–activated RTK cascade in glioblastoma "stem-like" cells (GSCs). In strong support of our experimental findings, we observed a significant correlation between elevated HIF activity and low *miR-218* expression in samples from patients with mesenchymal GBM; in contrast, no correlation was observed in proneural tumors. Collectively, our results identified an *miR-218*–RTK–HIF2α signaling axis that exists in highly necrotic, chemoresistant (mesenchymal) GBM. Finally, in mesenchymal GBM there is a functional association between *miR-218* expression and HIF activity, with RTK activation serving as the mechanistic link between the two.

CELL BIOLOGY

Significance

Despite measurable advances in cancer treatment, patients with glioblastoma multiforme (GBM) typically survive only 12–14 mo because of tumor recurrence. Tumor hypoxia has been associated with chemoresistance. We hypothesized that the pronounced repression of microRNA-218 (*miR-218*) observed in samples from patients with highly hypoxic and necrotic GBM contributes to this recurrent phenotype. We demonstrate here that mice harboring intracranial tumors with increased *miR-218* expression exhibit significantly reduced tumor burden and increased survival when challenged with the chemotherapeutic agent temozolomide. Moreover, low *miR-218* levels increase the expression of multiple components of the receptor tyrosine kinase signaling pathway, which promote the activation of hypoxia-inducible factor. The identification of the molecular bases for *miR-218*-mediated chemoresistance should promote the development of targeted therapies.

Author contributions: L.K.M., R.V.D., A.J.M., and M.C.S. designed research; L.K.M., N.S., V.M., S.S.L., and H.Z.I. performed research; S.V., P.L., J.D.L., J.N.R., and M.C.S. contributed new reagents/analytic tools; L.K.M., N.S., P.O.Z., P.S., Z.Z., S.R., A.J.M., and M.C.S. analyzed data; and L.K.M., B.K., and M.C.S. wrote the paper.

The authors declare no conflict of interest.

*This Direct Submission article had a prearranged editor.

[1]To whom correspondence should be addressed. E-mail: celeste2@mail.med.upenn.edu.

This article contains supporting information online at www.pnas.org/lookup/suppl/doi:10.1073/pnas.1314341111/-/DCSupplemental.

Results and Discussion

Tumors with high proliferation rates experience varying degrees of O_2 and nutrient availability, and conditions of extreme tumor ischemia can lead to necrosis. To identify important miRNAs associated with GBM ischemia, we compared two datasets of miRNA expression derived from The Cancer Genome Atlas Network (TCGA) database (Table S1): (*i*) miRNAs differentially expressed in samples from patients with GBM showing high or low levels of necrosis, and (*ii*) miRNAs significantly altered in GBM as compared with normal brain tissue. Among miRNAs shared by these groups, *miR-218* levels were significantly decreased in highly necrotic samples (Fig. 1*A* and Table S1). Highly necrotic patient samples with low *miR-218* expression also exhibited increased levels of *miR-210*, a previously characterized hypoxia-induced miRNA (11), validating the association between necrosis and hypoxia (Fig. 1*A*). Because *miR-218* expression is decreased substantially in GBM (9, 10) compared with normal brain tissue (Fig. 1 *B* and *C*), and *miR-218* levels are further repressed in patients with highly necrotic GBM, we investigated whether hypoxia modulates *miR-218* expression. Exposure to low O_2 levels inhibited *miR-218* levels modestly in most human GBM cell lines (Fig. S1); however, *miR-218* expression already is repressed significantly in these cells. Of note, *miR-218* is encoded within intronic sequences of *SLIT2* and *SLIT3* (12, 13), and these host genes are epigenetically silenced in various cancers, including GBM (14, 15).

Mesenchymal GBM subtypes exhibit extensive necrosis, whereas overexpression of a mesenchymal gene signature is correlated with poor prognosis in patients who have GBM (6). We therefore determined whether *miR-218* levels are repressed preferentially in the mesenchymal subtype. First, we used gene-expression signatures from two classifications methods (5, 6) to stratify TCGA GBM data. Consistent with previously published studies, the gene signature of

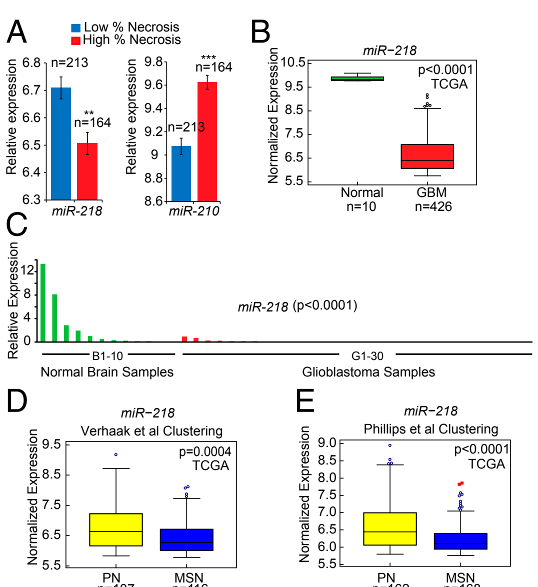

Fig. 1. Low *miR-218* expression is observed in highly necrotic, mesenchymal GBM. (*A*) *miR-218* and *miR-210* levels in samples from patients with GBM with high and low percentages of necrosis. (*B*) miR-218 expression in samples from patients with GBM and in normal brain tissue (TCGA) ($P < 0.0001$). (*C*) miR-218 expression analyzed by quantitative RT-PCR in samples from human GBM patient s obtained from the University of Pennsylvania (red; G1–G30) and in normal brain tissue (green; B1–B12). GBM patient sample G1 is normalized to a relative expression of 1 ($P < 0.0001$). (*D* and *E*) miR-*218* levels in mesenchymal (MSN) and proneural (PN) GBM subtypes according to two different published classification methods, the clustering of Verhaak et al. (6) ($P = 0.0001$) and that of Phillips et al. (5) ($P < 0.0001$). For all statistical analyses, *$P < 0.05$, **$P < 0.005$, ***$P < 0.0005$. Data are presented as mean ± SEM.

Verhaak et al. (6) stratified TCGA GBM samples ($n = 385$) into four subtypes (mesenchymal, proneural, neural, and classical), whereas the gene signature of Phillips et al. (5) classified these tumors into three subtypes (mesenchymal, proneural, and proliferative). We compared mesenchymal and proneural subtypes because these are the only common subgroups in the classification methods of Verhaak et al. and Phillips et al. Moreover, genomic analyses by other research groups have revealed the existence of two to four major hierarchical groupings of GBM (16, 17). Huse et al. (18) reviewed the different classification methods and suggest that the proneural and mesenchymal distinction is a common theme that emerges across different clustering approaches. Moreover, gene-expression patterns in these subtypes are mutually exclusive. Hierarchical clustering using an HIF signature indicated that mesenchymal GBM exhibit higher expression levels of HIF-regulated genes than do proneural tumors, as is consistent with increased hypoxia in mesenchymal GBM (Fig. S2). Our analysis using either classification method also revealed significant *miR-218* repression specifically in mesenchymal relative to proneural GBM, (Fig. 1 *D* and *E*), demonstrating that low *miR-218* expression is a characteristic feature of the highly necrotic and hypoxic mesenchymal GBM subset.

Mesenchymal GBM initially respond to treatment but often recur rapidly, producing highly chemoresistant tumors with very poor prognosis (6), and recurrent GBM from other subtypes shift toward a mesenchymal phenotype (5, 19). Although recent studies indicate that increased *miR-218* expression impacts cell viability in nasopharyngeal cancer and GBM cells (20, 21), a role for *miR-218* in conferring chemoresistance was not known. To test whether *miR-218* has such a role, we used a gain-of-function approach by restoring *miR-218* expression in GSCs or GBM cell lines. T3691 GSCs (22) stably expressing *miR-218* at levels typical of normal brain tissue (∼50 times higher than in GBM) (Fig. S3) were implanted intracranially into immunocompromised (*Nu*/*Nu*) mice. Interestingly, mice with orthotopic brain tumors derived from either T3691-SCR or T3691-218 cells revealed comparable tumor growth 12 d after transplantation (Fig. S4*A*). To test whether *miR-218* restoration sensitizes tumor cells to chemotherapeutic stress, we challenged transplanted animals at day 12 with temozolomide (TMZ), a widely used GBM chemotherapeutic agent (Fig. 2*A*). TMZ treatment resulted in significantly reduced growth in the *miR-218*–expressing (Tum-3691–218-TMZ) tumors, relative to Tum-3691-SCR-TMZ controls (Fig. 2*B*). Parallel studies performed with U87-SCR and U87-218 GBM cells displayed similar results (Fig. 2 *C* and *D*), indicating that *miR-218* expression increased the sensitivity of GSCs and GBM cells to TMZ treatment in vivo, resulting in tumor shrinkage.

To elucidate the basis of significant differences in tumor size upon *miR-218* re-expression, we first analyzed cell proliferation and death in GSC tumor xenografts from mice treated with TMZ. Based on cleaved caspase 3, Ki67, and phospho-Histone 3 immunostaining, we did not observe any striking differences in apoptotic cell death (Fig. S4*B*) or cell proliferation (Fig. S4 *C* and *D*) between control and *miR-218*–expressing GSC tumors in mice treated with TMZ. Similarly, Ki67 staining and TUNEL analysis also demonstrated that neither cell proliferation (Fig. S4*E*) nor apoptotic cell death (Fig. S4*F*) was altered between control and *miR-218*–expressing U87MG tumors in mice after TMZ treatment. Because of the decreased size of *miR-218*–expressing orthotopic lesions, we investigated the role of non-apoptotic cell death downstream of TMZ treatment. Loss of nuclear high-mobility group protein B1 (HMBG1) stain is a marker for autophagic, tumor cytolytic, or necrotic cell death (23–26), and we observed a significant reduction in nuclear HMGB1 staining in *miR-218*–expressing, TMZ-treated tumors in both orthotopic models (Fig. 2 *E* and *F*). Consistent with the in vivo tumor data, *miR-218*–expressing T3691 GSCs or U87MG cells treated with TMZ displayed similar results in vitro (Fig. S4 *G* and *H*). Furthermore, TMZ treatment failed to induce GBM cell apoptosis in other studies (27, 28), although alternative mechanisms of cell death were not explored. Our analyses

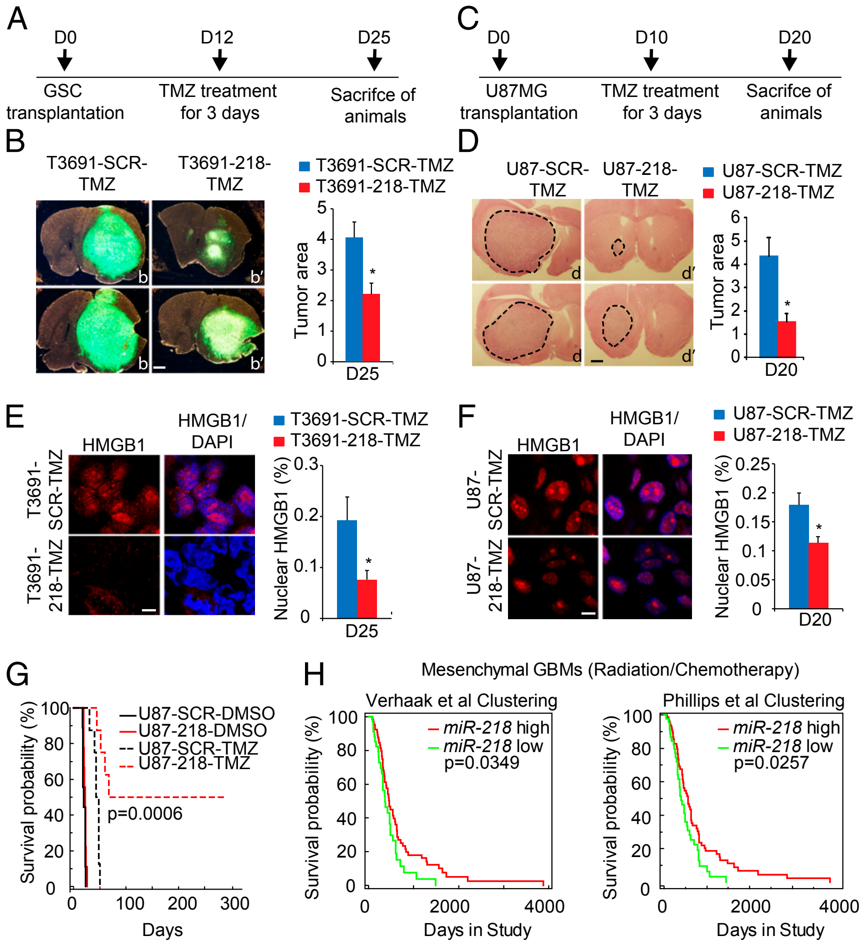

Fig. 2. *miR-218* increases GBM cell sensitivity to chemotherapeutic stress and affects orthotopic human brain tumor growth. (*A*) Schematic showing day of intracranial GSC transplantation (D0), day of TMZ treatment (D12), and day animals were killed (D25). (*B*, *Left*) Cryosections of GFP^{+} areas in GSC T3691-SCR/218 tumors treated with TMZ 12 d after intracranial injection and harvested 13 d later (D25). Representative images of Tum-3691-SCR -TMZ (*b*) and Tum-3691–218-TMZ (*b*′) are presented. (Scale bar: 1 mm.) n = 5 each. (*B*, *Right*) Quantification of GFP^{+} tumor area (in arbitrary units) of Tum-3691-SCR-TMZ, and Tum-3691–218-TMZ groups. (*C*) Schematic showing days of intracranial U87MG transplantation, TMZ treatment, and killing of animals. (*D*, *Left*) H&E sections of U87-SCR/218 tumors from animals treated with TMZ at 10 d after intracranial injection and killed 10 d later. Representative images of U87-SCR-TMZ (*d*) and U87-218-TMZ (*d*′) are presented. (Scale bar: 1 mm.) n = 4 each. (*D*, *Right*) Areas (in arbitrary units) of U87-SCR-TMZ and U87-218-TMZ tumors. (*E*) Immunofluorescent images and quantification of nuclear HMGB1 staining in orthotopic brain tumor sections from T3691-SCR-TMZ and T3691-218-TMZ groups. (Scale bar: 5 μm.) n = 4 each. (*F*) Representative images of U87-SCR-TMZ and U87-218-TMZ mouse brain sections depicting loss of nuclear HMGB1 in the U87-218-TMZ group. (Scale bar: 5 μm.) n = 4. (*G*) Kaplan–Meier curve demonstrating differences in survival of mice bearing U87-SCR orthotopic tumors relative to the U87-218 group, treated with DMSO or TMZ. n = 8 each. (*H*) Kaplan–Meier survival curve based on high and low *miR-218* expression in patients with mesenchymal GBM treated with radiation or chemotherapy [Verhaak et al. clustering (6), P = 0.0349; Phillips et al. clustering (5), P = 0.0257]. For all statistical analyses, *P < 0.05, * P < 0.005, ***P < 0.0005. Data are presented as mean ± SEM.

identify increased nonapoptotic cell death as a mechanism to explain the reduced tumor growth in *miR-218*–expressing tumors treated with TMZ.

A cohort of mice with orthotopic U87-SCR and U87-218 tumors was treated with DMSO or TMZ and monitored until they exhibited evidence of neurological deficits, at which time they were killed. Animals in the control U87-218-DMSO group had a modest change in median survival (22 d vs. 19 d in U87-SCR-DMSO mice) (Fig. 2*G*). However, mice bearing U87-SCR intracranial tumors lived an average of 45 d after TMZ treatment, and animals receiving both *miR-218* and TMZ exhibited a dramatic increase in survival: 50% failed to display any neurologic signs over 288 d (Fig. 2*G*). Remarkably, brain sections from these animals lacked any detectable tumor lesions (Fig. S4*I*). Of note, most of the established GBM cell lines exhibit a mesenchymal gene signature (6). We next examined whether *miR-218* levels correlate with prognosis in human GBM patients and observed that poor survival and rapid recurrence correlated with low *miR-218* expression specifically in patients with mesenchymal (but not proneural) GBM treated with radiation and chemotherapy (Fig. 2*H* and Fig. S5 *A–C*). Furthermore, the association between poor survival of patients with mesenchymal GBM and low *miR-218* expression was observed using either of the classification methods described above (Fig. 2*H* and Fig. S5 *A–C*) (5, 6). It is important to emphasize that mesenchymal GBM tumors are the most aggressive tumor type (6), and observing any survival differences within this group usually is challenging because of the rapid tumor recurrence.

Although we observed enhanced chemosensitivity with high *miR-218* expression (Fig. 2 *B*, *D*, and *G*), experimentally discerning the molecular basis of *miR-218*–mediated chemoresistance in mesenchymal and proneural subtypes is challenging. Bhat et al. (29) recently have shown that brain tumor cells grown as GSCs acquire proneural properties at both the genomic and epigenomic level. Most importantly, even GSCs derived from tumors with an intermediate to high mesenchymal gene signature shift toward the proneural phenotype (29). Therefore, establishing a role for *miR-218* in chemoresistance across the two GBM groups requires an extensive study using numerous, independently derived GSCs (from both subtypes); such study is warranted in the future.

To determine why *miR-218* expression is particularly repressed in mesenchymal GBM, we performed an inverse-correlation analysis between *miR-218* and putative *miR-218* targets identified in TCGA GBM gene-expression data using the bioinformatic program miRWalk. Among the top candidates identified in this analysis was a cluster of RTK signaling pathway members, including EGF receptor (*EGFR*), phospholipase C-γ1 (*PLCγ1*), phorphorhositide-B-IDnase, class 2, tar-polypeptide (*PIK3C2A*), and *v-raf murine sarcoma 3611 viral oncogene homolog* (*ARAF*), which we confirmed to be bona fide *miR-218*–regulated genes by mutating the *miR-218* seed sequence in their corresponding 3′ UTRs and testing their activity in standard luciferase reporter assays. In each case, *miR-218* expression reduced luciferase activity in a *miR-218* seed sequence-dependent manner (Fig. S6*A* and Table S2). Gene set enrichment analysis (GSEA) revealed a significant inverse correlation between the expression of *EGFR*, *PLCγ1*, or *ARAF* and *miR-218* in samples from patients with GBM (Fig. 3*A*). Furthermore, elevating *miR-218* expression in GBM cell lines by stable (Fig. 3*B*) or transient (Fig. S6*B*) transfection reduced the abundance of EGFR, PLCγ1, PIK3C2A, and ARAF proteins. Similarly, *EGFR*, *PLCγ1*, *PIK3C2A*, and *ARAF* transcript levels were decreased in GSC T3691-218

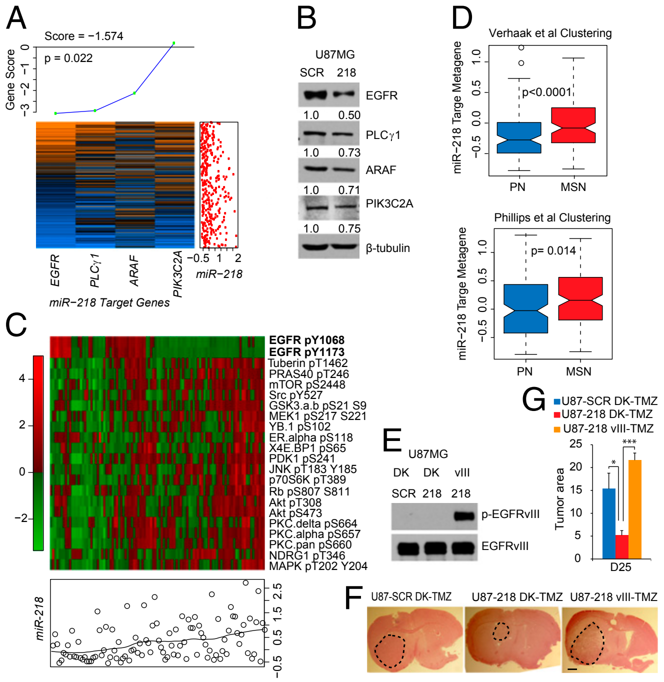

Fig. 3. Identification of multiple RTK pathway components as *miR-218* targets. (*A*) GSEA showing correlation between *miR-218* target genes and *miR-218* expression. The heatmap shows the expression of the target genes (columns) for each patient (rows) with orange indicating high expression, and blue indicating low expression. For each patient, the corresponding *miR-218* level is indicated in the dot plot to the right of the heatmap. The gene score for each gene is displayed in the plot above the heatmap along with the overall score and *P* value. Negative gene scores represent inverse correlation with *miR-218*. (*B*) Western blot showing the abundance of PLCγ1, EGFR, ARAF, and PIK3C2A proteins after stable *miR-218* expression in U87MG cells. The quantified value of protein expression represents the average of two experiments. β-Tubulin was used as a loading control. (*C*) Phospho-proteins from the RPPA database that significantly associate with *miR-218* expression are shown in the heatmap (red indicates high expression, and green indicates low expression). Each column is a sample, and each row is a phospho-protein. *miR-218* levels are indicated in the plot below the heatmap. (*D*) *miR-218* target metagene in mesenchymal (MSN) and proneural (PN) GBM subtypes, based on the clustering methods of both Verhaak et al. (6) and Phillips et al. (5). Shown are box-and-whisker plots of the distributions of the metagene values for patients in each subtype. (*E*) Western blot showing phosphorylation of EGFRvIII in U87-SCR or U87-218 cells transduced with EGFRvIII (vIII) or "dead kinase" (DK) constructs. (*F* and *G*) H&E sections and quantification of U87-SCR-DK, U87-218-DK, and U87-SCR-vIII tumors in mice treated with TMZ 12 d after intracranial injection and killed 13 d later. (Scale bar: 1 mm.) $n = 6$ each. For all statistical analyses, $^{*}P < 0.05$, $^{**}P < 0.005$, $^{***}P < 0.0005$. Data are presented as mean ± SEM.

orthotopic tumors with or without TMZ treatment (Fig. S6 *C* and *D*). Analysis of reverse-phase protein array (RPPA; TCGA) for phospho-proteomic data demonstrated that p-EGFR was the target that had the greatest inverse correlation with *miR-218* expression in samples from patients with GBM, supporting our hypotheses (Fig. 3*C*). Of note, low *miR-218* or high EGFR expression did not correlate with the downstream effectors of EGFR, indicating the complex role of RTK signaling in GBM. We also examined the effects of *miR-218* on RTK pathway activity in U87-SCR and U87-218 cells exposed to various stress conditions. Ischemic stress (serum-free medium + 0.5% O_2) combined with TMZ treatment reduced v-akt murine thymoma viral oncogene homolog 1 (AKT) and PRAS40 phosphorylation in *miR-218*–expressing cells, indicating that RTK signaling is inhibited upon *miR-218* introduction (Fig. S6*E*). Additionally, the levels of EGFR, PLCγ1, PIK3C2A, and ARAF expression were increased in GBM compared with normal brain tissue, as revealed by a combination of transcript analyses (Fig. S7*A*), examination of TCGA datasets (Fig. S7*B*), and immunohistochemical (IHC) staining of a GBM tissue array ($n = 40$) (Fig. S7*C*).

Because *miR-218* levels are more repressed in mesenchymal than in proneural GBM, we next determined whether the average expression of putative *miR-218* targets (designated the "*miR-218* target metagene") differs in these GBM subtypes. Both classification methods (5, 6) revealed a significant increase in the *miR-218* target metagene in mesenchymal relative to proneural GBM subtypes (Fig. 3*D*). Of note, *NF1* loss is a characteristic feature of mesenchymal GBM, consistent with high levels of RTK pathway activation (6), suggesting that low *miR-218* expression potentially contributes to a hyperactive RTK state.

The importance of EGFR is well established in GBM, but the specific roles of PLCγ1, PIK3C2A, and ARAF in these cells are not completely clear. EGF stimulation promotes PLCγ1 activation through its binding to the autophosphorylated EGFR Tyr992 residue in CHO cells (30), whereas PIK3C2A is a class II PI3K isoform acting upstream of mTOR overexpressed in oral

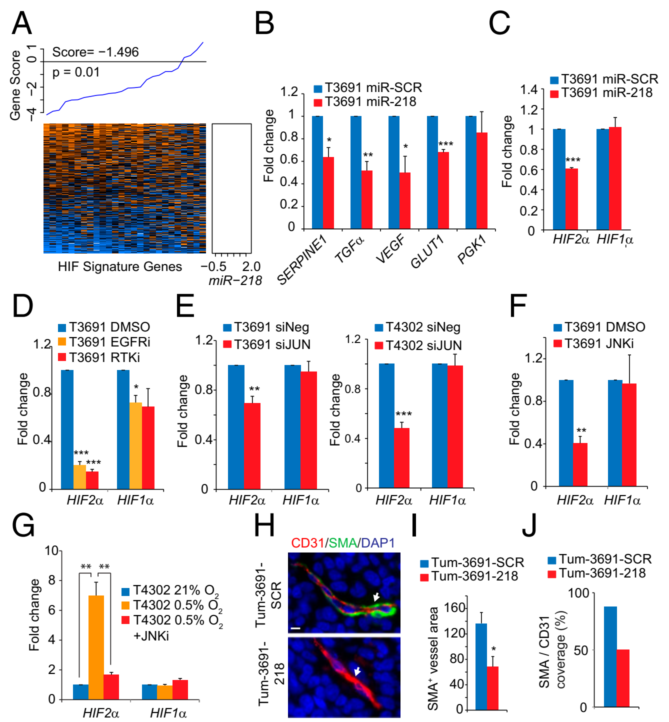

Fig. 4. *miR-218* modulates HIF activity through decreased RTK signaling. (*A*) GSEA demonstrating a negative correlation between an HIF signature and *miR-218* expression. The heatmap shows expression of an HIF signature gene (columns) for each patient (rows) with orange indicating high expression, and blue indicating low expression (for the list of HIF signature genes, see Fig. S2). For each patient, the corresponding expression level of *miR-218* is indicated in the dot plot to the right of the heatmap. The gene score for each gene is displayed in the plot above the heatmap along with the overall score and *P* value. Negative gene scores represent inverse correlation with *miR-218*. (*B* and *C*) HIF target genes (*B*) and *HIF1α* and *HIF2α* transcript levels (*C*) in T3691 GSC cells upon ectopic *miR-218* expression. (*D*) *HIF1α* and *HIF2α* transcript levels after specific EGFR inhibition (EGFRi) or general RTK inhibition (RTKi). (*E* and *F*) *HIF1α* and *HIF2α* mRNA levels upon siRNA-mediated suppression of jun proto-oncogene (c-JUN) (*E*) or JNK inhibition (JNKi) (*F*) in GSC cells. (*G*) Expression of *HIF1α* and *HIF2α* mRNA levels after exposure to 21% O_2, 0.5% O_2, or 0.5% O_2 + JNK inhibition (JNKi) for 24 h in GSC cells. (*H*) CD31 and SMA immunofluorescence in T3691-SCR and T3691-218 orthotopic brain tumor sections. (Scale bar: 5 μm.) $n = 4$. (*I*) Quantification of the SMA^+ area indicative of blood vessels and pericyte coverage, respectively, in T3691-SCR and T3691-218 sections. (*J*) Percentage of SMA^+ area coverage of total blood vessel area ($CD31^+$) in Tum-3691-SCR and Tum-3691-218 tumors. All expression studies depicted here were performed in triplicate. For all statistical analyses, $^{*}P < 0.05$, $^{**}P < 0.005$, $^{***}P < 0.0005$. Data are presented as mean ± SEM.

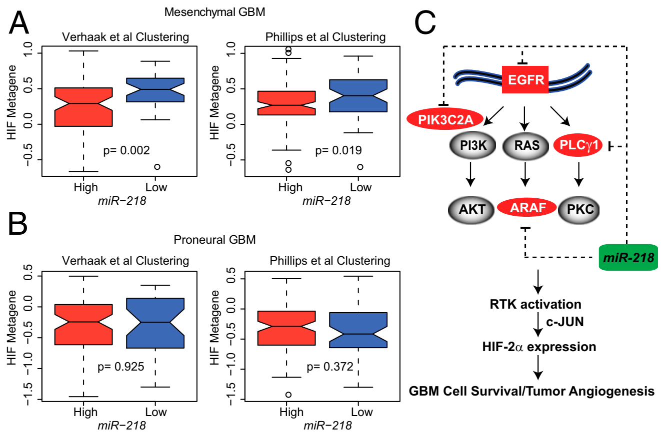

Fig. 5. *miR-218*–RTK–HIF signaling axis in mesenchymal GBM. (*A* and *B*) HIF metagene expression in patients with mesenchymal (*A*) and proneural (*B*) GBM with high or low *miR-218* levels based on the clustering methods of Verhaak et al. (6) and Phillips et al. (5) (TCGA data). Box-and-whisker plots show the distributions of the metagene values by *miR-218* status for patients in each subtype. (*C*) Schematic diagram depicting the effect of *miR-218* repression on multiple components of RTK signaling and thereby a cumulative impact on RTK and HIF activation, favoring GBM growth and tumor angiogenesis. Red and green correspond to increased expression and decreased expression, respectively.

squamous cell carcinoma (31, 32). ARAF, a member of the RAF kinase family, binds to v-raf murine sarcoma viral oncogene homolog B [BRAF (similar to CRAF)] and serves as a BRAF effector (33). Therefore, we investigated whether these direct targets contribute to *miR-218*–dependent chemosensitivity in vivo (Fig. 2*D*). If cumulative RTK activation is required to reverse the *miR-218*–mediated effects on tumor growth in vivo, reintroduction of individual *miR-218* targets may not be successful. Therefore, we used a plasmid encoding EGFRvIII to activate RTK signaling constitutively in *miR-218*–expressing cells, and a "dead kinase" (DK) construct as the control (Fig. 3*E*). U87-SCR or U87-218 cells transduced with lentiviruses expressing EGFRvIII or DK proteins were implanted intracranially into immunocompromised nude mice. Interestingly, the addition of EGFRvIII completely reversed the tumor shrinkage observed upon *miR-218* and TMZ treatment (Fig. 3 *F* and *G*), confirming the role of RTK signaling in the *miR-218*–mediated chemosensitivity of U87 tumors. These studies indicate that *miR-218* repression results in enhanced RTK activity in GBM, contributing to tumor cell survival under challenging microenvironmental conditions, including chemotherapeutic stress and severe hypoxia.

Tumor hypoxia has been linked to chemoresistance, and recent studies demonstrate that low O_2 concentrations maintain tumor stem cells in an undifferentiated state (34, 35). HIFs (and HIF2α in particular) promote GSC self-renewal, proliferation, and survival (36). Furthermore, high *HIF2α* levels correlate with poor survival in patients with glioma (36). Previous reports demonstrated that multiple components of RTK signaling promote HIF expression, with consequent effects on tumor angiogenesis and response to therapy (37–39). GSEA revealed that low *miR-218* abundance is significantly associated with an enrichment of HIF signature genes in human GBM samples (Fig. 4*A*), as is consistent with our hypothesis that low *miR-218* promotes HIF activation through RTK signaling. To test this premise, we stably expressed *miR-218* in T3691 and T4302 GSCs and observed reduced transcription of HIF2α-regulated genes (e.g., *TGF-α*, *VEGF*, and *GLUT1*); in contrast, HIF1α-regulated genes (*PGK1*, *PDK1*, and *ALDOA)* were not inhibited by *miR-218* treatment (Fig. 4*B* and Fig. S8*A*). Consistently, the introduction of *miR-218* inhibited *HIF2α*,but not *HIF1α* mRNA levels in T3691 (Fig. 4*C*) and T4302 GSCs (Fig. S8*B*). To test whether this effect was dependent on RTK activation in cells with low *miR-218* expression, we used RTK inhibitors and analyzed the accumulation of HIFα isoforms and their downstream target genes. Although the abundance of both *HIFα* transcripts was reduced by RTK inhibition, *HIF2α* levels again were significantly lower than those of *HIF1α* (Fig. 4*D*). Moreover, HIF2α–regulated target genes (*SERPINE1* and *TGF-α*) were preferentially repressed by RTK inhibition (Fig. S8 *C* and *D*), revealing a mechanism whereby low *miR-218* expression promotes tumor cell survival in GBM.

To determine how *HIF2α* is transcriptionally regulated by RTKs in GBM, we analyzed its promoter region for transcription factors controlled by RTK signaling pathways and identified jun proto-oncogene (c-JUN) as a potential candidate (ENCODE; http://genome.ucsc.edu/cgi-bin/hgGateway). Interestingly, siRNA-mediated suppression of c-JUN inhibited *HIF2α* but not *HIF1α* expression in T3691 and T4302 GSCs (Fig. 4*E* and Fig. S8 *E* and *F*). Because c-JUN is activated mainly through JNK signaling (40), we assessed the impact of JNK inhibition on *HIFα* expression and observed reduced *HIF2α* but not *HIF1α* mRNA levels in T3691 and T4302 GSCs (Fig. 4*F* and Fig. S8 *G* and *H*). Because *HIF2α* expression is transcriptionally enhanced in hypoxic GSCs (36), we next investigated whether *HIF2α* stimulation is JNK dependent and determined that JNK inhibition significantly attenuated hypoxic induction of *HIF2α* but not of *HIF1α* (Fig. 4*G* and Fig. S8*I*). Therefore, a molecular link between *miR-218*–mediated RTK activation and *HIF2α* expression involves JNK signaling via c-JUN. It is important to note that *HIF2α* was not predicted to be a direct *miR-218* target by multiple bioinformatics analyses, indicating that *miR-218* regulation of *HIF2α* is indirect, presumably through RTK signaling pathways.

Because hypoxia promotes tumor angiogenesis (41), a characteristic feature of highly aggressive mesenchymal GBM, we characterized vessel density and pericyte coverage in tumor blood vessels. Although no difference in vascular area (based on $CD31^+$ immunostaining) was observed in T3691-SCR and T3691-218 tumors (Fig. 4*H* and Fig. S8 *J* and *K*), pericyte coverage [smooth muscle actin (SMA)-positive cells] was significantly reduced in the T3691-218 tumors (arrows in Fig. 4*H*). Quantification of SMA staining (Fig. 4 *I* and *J)* indicated that vessel maturation is inhibited in T3691-218 tumors. This effect of *miR-218* on tumor angiogenesis is consistent with the impact of reduced HIF2α activity in other tumor model systems (42, 43). Cheng et al. (44) recently demonstrated that GSCs can transdifferentiate into pericytes, and delineating a role for an *miR-218*–RTK–HIF2α signaling axis in this process is warranted in the future. Taken together, our studies indicate that low *miR-218* expression promotes RTK and HIF activation in mesenchymal GBM, contributing to chemoresistance and tumor vascularization.

Finally, because *miR-218* levels were further reduced in mesenchymal relative to proneural GBM, we analyzed the functional significance of an *miR-218*–RTK–HIF signaling axis in these GBM subtypes. Samples from patients with mesenchymal or proneural GBM were divided into two groups ("high" and "low") based on *miR-218* expression. Interestingly, samples from patients with mesenchymal GBM with low *miR-218* levels exhibited elevated expression of an HIF metagene (Fig. 5*A*), supporting our contention that low *miR-218* increases HIF activation. Similarly, GSEA revealed an inverse correlation between an HIF gene signature and *miR-218* expression in mesenchymal GBM (Fig. S9*A*). Importantly, no significant association was observed between *miR-218* levels and the HIF metagene (Fig. 5*B*) or the HIF gene signature (Fig. S9*B*) in proneural GBM. We concluded that the *miR-218*–RTK–HIF2α signaling pathway operates preferentially in highly aggressive mesenchymal GBM.

Although the use of miRNAs for therapeutic intervention is still in its earliest phases of development, our study suggests that the combined use of synthetic *miR-218* with chemotherapeutic agents could be beneficial for patients who have GBM, particularly those with mesenchymal tumors. Most importantly, we demonstrate that *miR-218* functions as a tumor suppressor in GBM by targeting multiple components of RTK signaling pathways

(Fig. 5*C*) and reveal mechanisms whereby low *miR-218* expression promotes GBM tumorigenesis.

Materials and Methods

We obtained formalin-fixed paraffin-embedded tissues from 30 GBM cases (World Health Organization grade IV/IV) and 12 controls from the Department of Pathology and Laboratory Medicine, University of Pennsylvania. GBM blocks contained more than 95% tumor cells. Controls consisted of temporal lobectomy specimens obtained from patients with intractable epilepsy and showed histopathologic evidence of mild to focally moderate gliosis but no lesions. GBM patients ranged in age from 24–89 y, with a median age of 63 y. Control patients ranged in age from 22–61 y, with a median age of 38 y.

Other information on materials and methods is described in *SI Materials and Methods*.

ACKNOWLEDGMENTS. We thank Hongwei Yu for histological preparations, Paul Hallberg for assistance with cell sorting, and the members of the M.C.S. laboratory for helpful discussions and comments. This work was funded by the Howard Hughes Medical Institute and National Institutes of Health Grant CA104838. M.C.S. is an investigator of the Howard Hughes Medical Institute.

1. Simon MC, Keith B (2008) The role of oxygen availability in embryonic development and stem cell function. *Nat Rev Mol Cell Biol* 9(4):285–296.
2. Stupp R, et al. (2009) Neoadjuvant chemotherapy and radiotherapy followed by surgery in selected patients with stage IIIB non-small-cell lung cancer: A multicentre phase II trial. *Lancet Oncol* 10(8):785–793.
3. Brat DJ, et al. (2004) Pseudopalisades in glioblastoma are hypoxic, express extracellular matrix proteases, and are formed by an actively migrating cell population. *Cancer Res* 64(3):920–927.
4. Cooper LA, et al. (2012) The tumor microenvironment strongly impacts master transcriptional regulators and gene expression class of glioblastoma. *Am J Pathol* 180(5): 2108–2119.
5. Phillips HS, et al. (2006) Molecular subclasses of high-grade glioma predict prognosis, delineate a pattern of disease progression, and resemble stages in neurogenesis. *Cancer Cell* 9(3):157–173.
6. Verhaak RG, et al.; Cancer Genome Atlas Research Network (2010) Integrated genomic analysis identifies clinically relevant subtypes of glioblastoma characterized by abnormalities in PDGFRA, IDH1, EGFR, and NF1. *Cancer Cell* 17(1):98–110.
7. Esquela-Kerscher A, Slack FJ (2006) Oncomirs - microRNAs with a role in cancer. *Nat Rev Cancer* 6(4):259–269.
8. Stahlhut Espinosa CE, Slack FJ (2006) The role of microRNAs in cancer. *Yale J Biol Med* 79(3-4):131–140.
9. Silber J, et al. (2008) miR-124 and miR-137 inhibit proliferation of glioblastoma multiforme cells and induce differentiation of brain tumor stem cells. *BMC Med* 6:14.
10. Godlewski J, et al. (2008) Targeting of the Bmi-1 oncogene/stem cell renewal factor by microRNA-128 inhibits glioma proliferation and self-renewal. *Cancer Res* 68(22): 9125–9130.
11. Kulshreshtha R, et al. (2007) A microRNA signature of hypoxia. *Mol Cell Biol* 27(5): 1859–1867.
12. Davidson MR, et al. (2010) MicroRNA-218 is deleted and downregulated in lung squamous cell carcinoma. *PLoS ONE* 5(9):e12560.
13. Tie J, et al. (2010) MiR-218 inhibits invasion and metastasis of gastric cancer by targeting the Robo1 receptor. *PLoS Genet* 6(3):e1000879.
14. Dickinson RE, et al. (2004) Epigenetic inactivation of SLIT3 and SLIT1 genes in human cancers. *Br J Cancer* 91(12):2071–2078.
15. Dallol A, et al. (2003) Frequent epigenetic inactivation of the SLIT2 gene in gliomas. *Oncogene* 22(29):4611–4616.
16. Freije WA, et al. (2004) Gene expression profiling of gliomas strongly predicts survival. *Cancer Res* 64(18):6503–6510.
17. Vital AL, et al. (2010) Gene expression profiles of human glioblastomas are associated with both tumor cytogenetics and histopathology. *Neuro-oncol* 12(9):991–1003.
18. Huse JT, Phillips HS, Brennan CW (2011) Molecular subclassification of diffuse gliomas: Seeing order in the chaos. *Glia* 59(8):1190–1199.
19. Tso CL, et al. (2006) Primary glioblastomas express mesenchymal stem-like properties. *Mol Cancer Res* 4(9):607–619.
20. Alajez NM, et al. (2011) MiR-218 suppresses nasopharyngeal cancer progression through downregulation of survivin and the SLIT2-ROBO1 pathway. *Cancer Res* 71(6): 2381–2391.
21. Xia H, et al. (2013) MiR-218 sensitizes glioma cells to apoptosis and inhibits tumorigenicity by regulating ECOP-mediated suppression of NF-κB activity. *Neuro-oncol* 15(4):413–422.
22. Eyler CE, et al. (2011) Glioma stem cell proliferation and tumor growth are promoted by nitric oxide synthase-2. *Cell* 146(1):53–66.
23. Gdynia G, et al. (2010) Danger signaling protein HMGB1 induces a distinct form of cell death accompanied by formation of giant mitochondria. *Cancer Res* 70(21):8558–8568.
24. Ito N, et al. (2007) Cytolytic cells induce HMGB1 release from melanoma cell lines. *J Leukoc Biol* 81(1):75–83.
25. Scaffidi P, Misteli T, Bianchi ME (2002) Release of chromatin protein HMGB1 by necrotic cells triggers inflammation. *Nature* 418(6894):191–195.
26. Thorburn J, et al. (2009) Autophagy regulates selective HMGB1 release in tumor cells that are destined to die. *Cell Death Differ* 16(1):175–183.
27. Hegi ME, et al. (2005) MGMT gene silencing and benefit from temozolomide in glioblastoma. *N Engl J Med* 352(10):997–1003.
28. Oliva CR, et al. (2010) Acquisition of temozolomide chemoresistance in gliomas leads to remodeling of mitochondrial electron transport chain. *J Biol Chem* 285(51): 39759–39767.
29. Bhat KP, et al. (2013) Mesenchymal differentiation mediated by NF-κB promotes radiation resistance in glioblastoma. *Cancer Cell* 24(3):331–346.
30. Nogami M, et al. (2003) Requirement of autophosphorylated tyrosine 992 of EGF receptor and its docking protein phospholipase C gamma 1 for membrane ruffle formation. *FEBS Lett* 536(1-3):71–76.
31. Krag C, Malmberg EK, Salcini AE (2010) PI3KC2α, a class II PI3K, is required for dynamin-independent internalization pathways. *J Cell Sci* 123(Pt 24):4240–4250.
32. Chakraborty S, Mohiyuddin SM, Gopinath KS, Kumar A (2008) Involvement of TSC genes and differential expression of other members of the mTOR signaling pathway in oral squamous cell carcinoma. *BMC Cancer* 8:163.
33. Rebocho AP, Marais R (2013) ARAF acts as a scaffold to stabilize BRAF:CRAF heterodimers. *Oncogene* 32(26):3207–3212.
34. Chou CW, et al. (2012) Tumor cycling hypoxia induces chemoresistance in glioblastoma multiforme by upregulating the expression and function of ABCB1. *Neuro-oncol* 14(10):1227–1238.
35. Kolenda J, et al. (2011) Effects of hypoxia on expression of a panel of stem cell and chemoresistance markers in glioblastoma-derived spheroids. *J Neurooncol* 103(1): 43–58.
36. Li Z, et al. (2009) Hypoxia-inducible factors regulate tumorigenic capacity of glioma stem cells. *Cancer Cell* 15(6):501–513.
37. Lu Y, Liang K, Li X, Fan Z (2007) Responses of cancer cells with wild-type or tyrosine kinase domain-mutated epidermal growth factor receptor (EGFR) to EGFR-targeted therapy are linked to downregulation of hypoxia-inducible factor-1alpha. *Mol Cancer* 6:63.
38. Xu L, et al. (2010) Epidermal growth factor receptor regulates MET levels and invasiveness through hypoxia-inducible factor-1alpha in non-small cell lung cancer cells. *Oncogene* 29(18):2616–2627.
39. Zhong H, et al. (2000) Modulation of hypoxia-inducible factor 1alpha expression by the epidermal growth factor/phosphatidylinositol 3-kinase/PTEN/AKT/FRAP pathway in human prostate cancer cells: Implications for tumor angiogenesis and therapeutics. *Cancer Res* 60(6):1541–1545.
40. Meng Q, Xia Y (2011) c-Jun, at the crossroad of the signaling network. *Protein Cell* 2(11):889–898.
41. Krock BL, Skuli N, Simon MC (2011) Hypoxia-induced angiogenesis: Good and evil. *Genes Cancer* 2(12):1117–1133.
42. Skuli N, et al. (2009) Endothelial deletion of hypoxia-inducible factor-2alpha (HIF-2alpha) alters vascular function and tumor angiogenesis. *Blood* 114(2):469–477.
43. Skuli N, et al. (2012) Endothelial HIF-2α regulates murine pathological angiogenesis and revascularization processes. *J Clin Invest* 122(4):1427–1443.
44. Cheng L, et al. (2013) Glioblastoma stem cells generate vascular pericytes to support vessel function and tumor growth. *Cell* 153(1):139–152.